ISSN 1505-4675

Technical Sciences

17(2) 2014

Biosystems Engineering
Civil Engineering
Environmental Engineering
Geodesy and Cartography
Information Technology
Mechanical Engineering
Production Engineering

Technical Sciences 17(2), 2014, 149–163

INFLUENCE OF MESH REFINEMENT ON RESULTS OF ELASTIC-PLASTIC FEM ANALYSIS

***Paweł Szabracki*[1], *Tomasz Lipiński*[2]**

Chair of Material and Machinery Technology
University of Warmia and Mazury in Olsztyn

Received 29 October 2013, accepted 22 April 2014, available on line 4 May 2014

K e y w o r d s: FEM analysis, local mesh refinement, elastic-plastic deformation, error optimization.

A b s t r a c t

To improve fitting of numerical results to experimental data, in the past, distances between nodes were decreased for whole mesh. A typical mesh generator for Finite Element Method (FEM) analysis ensures possibility to decrease distances between nodes for edges or surfaces of described geometries. Influence of local mesh refinement for a flat and round tensile specimen on fitting of numerical tensile simulation results to experimental data was presented in the paper. Local mesh refinement was performed for areas with the error values higher than threshold value. First iteration of flat and round mesh refinement has to improved correlation of numerical and experimental data with acceptable increase of mesh file size. Similar observations have been made for the second iteration of the flat specimen mesh. On the basis of analysis, shown that second iteration of round mesh refinement caused crucial increase of mesh file size and computation time with negligible fitting improvement.

Introduction

Finite Element Method (FEM) analysis make possible mechanical, thermal acoustic and other calculations for different geometries not restricted to normalized shapes (BÉCACHE et al. 2005, BELL et al. 2006, DUARTEM et al. 2013, DUMONT et al. 2013, KŁYSZ et al. 2013, KUHL et al. 2013, KUHL et al. 2013, MIAZIO, ZBOIŃSKI 2013, PERDUTA, PUTANOWICZ 2013, ROSSILLON, MEZIERE 2010, SZABRACKI 2012).Geometrical model in FEM analysis has to be defined with discrete elements. Preparation of the mesh describing geometrical model, built on discrete elements is very important for calculation accuracy. Typically, to build discrete model of analyzed geometry, nodes, edges, plane figures and

* Correspondence: Pawel Szabracki, Katedra Technologii Materiałów i Maszyn, Uniwersytet Warmińsko-Mazurski, ul. Oczapowskiego 11, 10-719 Olsztyn, tel.: +48 89 523 38 55, e-mail: pawel.szabracki@uwm.edu.pl

polyhedrons are used. Geometrical edges and planes have to be divided for smaller parts to achieve discrete elements. Ends of the smaller parts are called as nodes. Connected nodes are defined as edges. Connected edges form plane figures. Connected plane figures form polyhedron. The most commonly used plane figures are triangles and rectangles. On the basis of plane figures, the most commonly used three-dimensional solids used to build discrete model of analyzed geometry are tetrahedron and cuboids.

Most commonly used methods to generate mesh base on maximal distance between nodes or number of element along edge. Typical software used for preprocessing enables to define specific distance between nodes for different areas of the geometry. Literature presents three main refinement methods. *h-refinement* method is focused on the local refinement and/or coarsening of a mesh. Second method, *r-refinement* method, is used to relocate or move a mesh. *p-refinement* method is focused on local varying the polynomial degree of the basis. These strategies can be used singly or in combination. *r-refinement* is usually useful with transient problems, where elements move according to described phenomena. Many researchers improve methods of mesh refinement to modify initial mesh on the basis of error distribution or other criterion (ALEXA 2002, BABUSKA et al. 1995, BABUSKA, RHEINBOLDT 1978, BERN et a. 1999, CLARK et al. 1994, DUNCAN 1998, FLAHERTY et al. 1989, MIAZIO, ZBOIŃSKI 2013, NICOLAS, FOUQUET 2013, PERDUTA, PUTANOWICZ 2013).

Current literature trends confirms application of different refinement algorithms for practical calculations (BÉCACHE et al. 2005, BELL et al. 2006, DUARTEM et al. 2013, DUMONT et al. 2013, KOSTOFF et al. 2013, KUHL et al. 2013), what was also made for tensile test simulation in the paper.

On the basis of FEM analysis, stress and strain distributions for flat and round tensile specimens were analyzed. To perform Finite Element Analysis (FEA) of tensile specimens, meshes of the specimens has to be prepared. Mesh generation on the basis of maximal distance between nodes or number of element on the edge of geometry is not sufficient to properly describe nonlinear behavior in those areas. Nonlinear behavior requires mesh with small distance between nodes. Usually, nonlinear behavior occurs in small areas of analyzed geometry. Mesh refinement on the basis of edge and surfaces of geometry is usually not sufficient for 3D geometries. Definition of distance between nodes for whole mesh like for areas with nonlinear behavior induce creation of large mesh file with huge amount of nodes without practical importance for calculation results. Many nodes need a lot of time and computer resources for calculations and the vast majority of nodes in areas with elastic behavior are useless. As results of homogenous mesh refinement we obtain crucial increase of calculation time and many nodes useless for performed analysis. Local mesh refinement methods based on error distribution provide tools and methodology

to optimize number of nodes in mesh for performed analysis. Concerning applicability of different refinement methods, *h*-refinement methods was choosing. Methodology, which implies the use of tetrahedral and pyramids to connect the zones of different level of refinement (NICOLAS, FOUQUET 2013), was used. Literature does not present any information about influence of tensile test specimen's local refinement on the accuracy of tensile test simulation results. Especially for X2CrNiMoN25-7-4 super duplex stainless steel used to build responsible constructions working with danger substances.

FEA are cheaper than manufacturing and testing of machine and construction prototypes. To analyze complex geometries, large amount of computer hardware has to be used. Mesh refinement in specific areas, where error is to high, is important for those practical analysis. Local mesh refinement ensure optimal supplement of the mesh with additional nodes. Areas of the mesh not important for performed analysis are not modified. Concerning practical application of different numerical analysis (BÉCACHE et al. 2005, BELL et al. 2006, DUARTEM et al. 2013, DUMONT et al. 2013, KOSTOFF, CUMMINGS 2013, KUHL et al. 2013, SZABRACKI 2012, SZABRACKI et al. 2012, SZABRACKI, LIPIŃSKI 2013), aim of performed analysis was to determine influence of double mesh refinement of flat and round tensile specimen on the fitting of numerically calculated to experimental data. Results allow to define influence of refinement iterations on the accuracy of numerical results. Simple geometry (normalized round and flat tensile specimen) allows to verify methodology and will be background for usage of a presented methodology for more complex, real geometries.

Research methodology

According to standard PN-EN ISO 6892-1, tensile test can be performed for specimens with round and rectangular cross section. Tensile specimens with round and rectangular cross section are used due to the different forms of semi-finished and metallurgical products. Flat specimens with rectangular cross section are used for thin plates. Specimens with round cross sections are used for thick plates and rods. Experimentally tested tensile specimens were made of X2CrNiMoN25-7-4 super duplex stainless steel. Tensile specimens with rectangular cross section according to Figure 1 were prepared from 5 mm thick plate (water jet with abrasive cutting).

In the paper, local mesh refinement of round and rectangular specimens used for tensile test simulation were performed. Diameter of working part in round specimen is 8 mm. Rectangular cross section of flat specimen is equal 5×10 mm. The FEM simulation results were compared with experimental

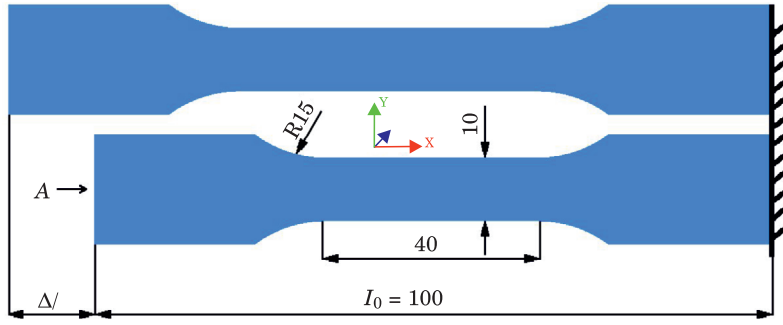

Fig. 1. Schematic presentation of tensile test simulation

tensile curve for flat (rectangular cross section) specimen (Fig. 1). Round tensile specimen was not experimentally tested. The FEM simulation results confirms possibility of usage FEA regardless of the geometry. Important part of a finite element analysis is the discrete model of analyzed geometry preparation. According to the methodology of tensile test simulation presented in the paper (SZABRACKI et al. 2012), analyzed in this paper simulations were performed for elastic and plastic deformations until Ultimate Tensile Strength (UTS) reached. Failure of the numerical specimen were defined when stresses in mesh reach UTS value. Practically, for experimental test UTS value was reached, visible neck creation starts.

FEM calculations were performed on the basis of Code Aster solver (TAYLOR 1999).The solver was developed for nuclear installations analysis. Open source code allows to improve the solver by different researchers and programmers around the world. Main advantage of the code is wide range of applications for mechanical, thermal, metallurgical and acoustic analysis.

Elastic-plastic behavior of X2CrNiMoN25-7-4 super duplex stainless steel was defined according to isotropic hardening model (1) described and presented in previous works (ALEXA 2002, NICOLAS, FOUQUET 2013, SZABRACKI et al. 2012).

$$R(p) = \sigma_i + \frac{\sigma_{i+1} - \sigma_i}{p_{i+1} - p_i}(p - p_i) \tag{1}$$

where:

$p_i = \varepsilon_i - \frac{\sigma_i}{\mathrm{E}}$

E – Young modulus

σ_i – stresses in point i of the experimental tensile curve [MPa]

ε_i – strains in point i of the experimental tensile curve [MPa]

Initial mesh, describing tensile specimen with rectangular cross section, shown in Figure 2a). The Mesh contains triangles (2D) and tetrahedrons (3D). The maximal distance between nodes was 2.5 mm. For nonlinear areas of the flat specimen geometry (connection of working and handling part of the specimen), maximal distance between nodes decreased to 1 mm. Mesh prepared according to described above criteria contains 2,054 nodes, 272 edges, 2,936 triangles and 7,298 tetrahedrons (Fig. 2a). Maximal distance between nodes in round tensile specimen decreased to 1.5 mm for handling part and 1 mm for other parts of the specimen. The maximal distance between nodes decrease has increased number of nodes in the mesh. Mesh of the round tensile specimen contains 5,238 nodes, 352 edges, 70,114 triangles and 19,642 tetrahedrons (Fig. 2b). Described above changes in mesh generation condition caused changes of the mesh files size. The file size of flat tensile specimen mesh is equal 312 KB and the file size of round tensile specimen mesh is equal to 782 KB.

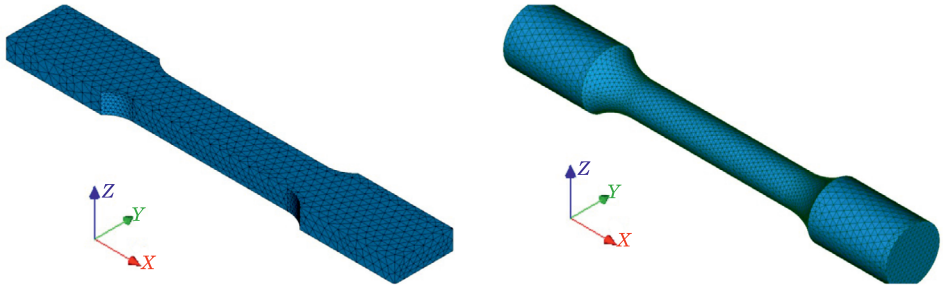

Fig. 2. Initial mesh of *a*) flat and *b*) round tensile specimen

Tensile test simulation was performed according to methodology described in the paper (SZABRACKI et al. 2012) with linear displacement of surface A (Fig. 1) along – x axis. Velocity of A surface displacement was 0.5 mm/s. Iteration step was changing during simulation. Nonlinear behavior of the material in plastic deformation areas causes decrease of iteration steps to achieve convergence threshold value. 20 convergence iterations were used as maximal acceptable number of convergence steps. If it was not enough to achieve threshold convergence value, the A surface step was decreased 2 times until convergence criterion was fulfilled. For elastic deformation area, iteration step was 0.5 mm. When highest stresses in mesh were almost equal to Yield Strength, iteration step decreased to 0.1 mm. When UTS reached, error distribution in the plane mesh elements (K) indicates the estimator of error (noted (Ω)) was defined as being the quadratic average of the site indicators of

error ($\eta(K)$) (3) (NICOLAS, FOUQUET 2013). This kind of error estimation allow to detect significant changes of calculated values (stresses, strains or others) for neighboring plane elements. Used estimator is an explicit estimator of error utilizing the residues of the balance equations and the jumps of the normal stresses to the application interfaces (NICOLAS, FOUQUET 2013). Contrary to the Zhu-Zienkiewicz estimator (AINSWORTHET et al. 1989), which uses a techniques of smoothing of the stresses a posteriori. In this case, areas with significant values evolution for neighboring nodes will be refined without modification of not significant areas.

$$\eta(\Omega) = [\sum_{K \in T} \eta(K)^2]^{\frac{1}{2}} \tag{3}$$

$$\eta(\Omega)_{\text{rel}} = \eta(\Omega)_{\min} + \eta_{\text{rel}}(\eta(\Omega)_{\max} - \eta(\Omega)_{\min}) \tag{4}$$

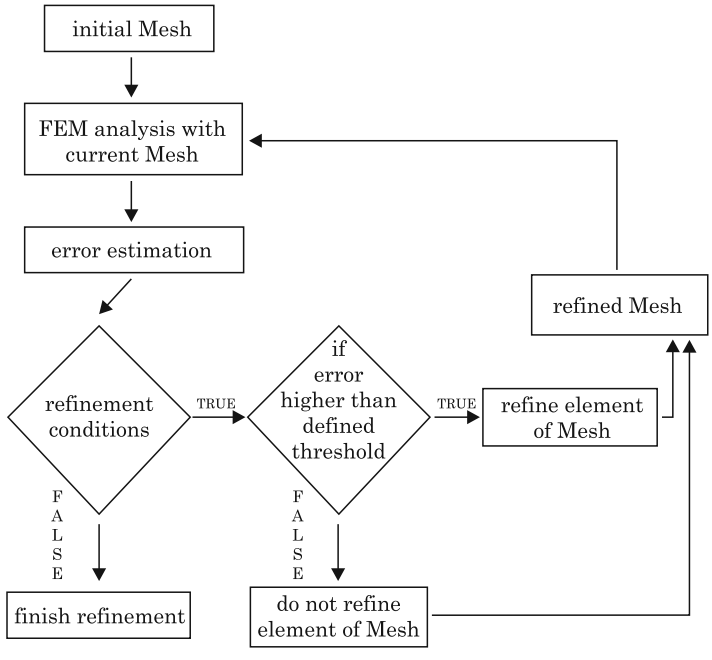

Fig. 3. Mesh refinement algorithm

For areas with error higher than threshold value, mesh refinement based on the error distribution (NICOLAS, FOUQUET 2013) in the plane mesh elements was performed. Threshold value for mesh refinement was calculated according to formula (4) with 10% relative error η_{rel} (NICOLAS, FOUQUET 2013). This value allows significantly rebuilding the mesh after each iteration step. Higher values of relative error require more refinement iteration steps. For more

complex geometries, higher relative error can be required. Normalized tensile specimens not require small steps of mesh refinement.

The mesh refined according to presented methodology was used for next iteration of tensile test simulation. Influence of mesh refinement on experimental tensile curve fitting was analyzed according to prepared algorithm (Fig. 3). For cases where more than two iterations will be needed, mesh refinement ending criterion was used, to achieve less than 2% increase of the correlation coefficient value. Due to the significant consumption of computing resources, crucial increase of the mesh file size resulting significant increase of computation time without significant improvement of the results quality were considered as condition terminating the algorithm. In the present case, more than two mesh refinement iterations was not used.

Stress and strains distributions (numerically calculated tensile curve) at the point of symmetry for round and flat tensile specimen were compared with experimental tensile curve. Pearson's correlation coefficient (5) was used to describe fitting of numerical results to experimental data (TAYLOR 1999).

$$r_{xy} = \frac{cov(xy)}{\sigma_x \sigma_y} \tag{5}$$

where:

$$\sigma_x = \sqrt{\frac{\sum_{i=1}^{n}(x_i - \bar{x})^2}{n}},$$

$$\sigma_y = \sqrt{\frac{\sum_{i=1}^{n}(y_i - \bar{y})^2}{n}}.$$

Results and analysis

Table 1 presents number of elements (0D-3D) used to build meshes of flat and round tensile specimen for initial state and after mesh refinement.

Table 1

Mesh 0D – 3D elements for different samples and refinement iterations

Iteration	Flat sample				Round sample			
	Nodes	1D	2D	3D	Nodes	1D	2D	3D
0 – Initial Mesh	2,054	272	2,936	7,298	5,238	352	7,014	19,642
1 – First refinement	7,193	372	6,656	32,179	16,732	416	14,662	76,353
2 – Second refinement	33,439	459	15,108	174,631	79,686	497	28,476	428,603

The size of flat specimen files increases from 312 KB to 2.6 MB after first refinement. The round specimen files size increases from 782 KB to 6.1 MB. Figure 4a presents error distribution for flat specimen before refinement, when UTS reached in working part. Similar error distribution in round specimen presents Figure 4b. Maximal error value, calculated according formula (3) for flat specimen is 1,285. For round specimen 918. Maximal error values are not located in the middle part of working area because of symmetry conditions and restrictions of error estimation model (3) (NICOLAS, FOUQUET 2013). According to error distribution (Fig. 4) and presented methodology, refined meshes of flat (Fig. 5a) and round (Fig. 5b) specimen were prepared.

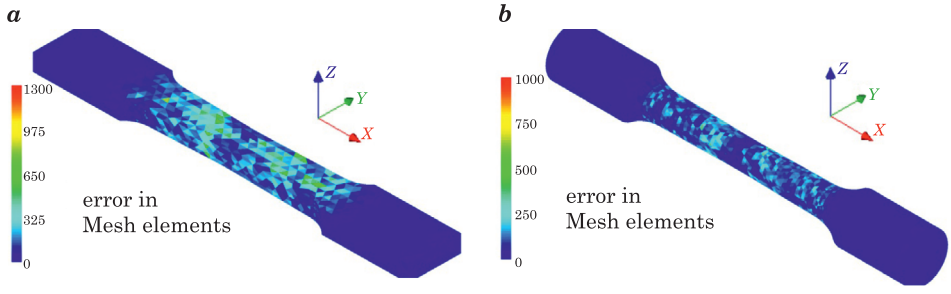

Fig. 4. Error distribution for initial mesh of *a*) flat and *b*) round specimen

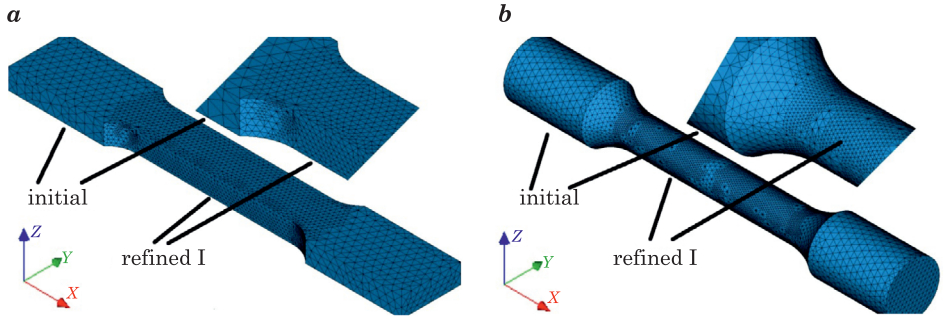

Fig. 5. Mesh after first mesh refinement iteration of *a*) flat and *b*) round specimen

On the basis of local mesh refinement method, number of nodes in middle part of flat specimen was increased (Fig. 5a – Refined I). Handling part of the mesh was not modified in this refinement iteration (Fig. 5a – Initial). Difference between handling and working part of the specimen allow to compare mesh element size before and after refinement. Mesh refinement presented in the specimen's surface is the same for whole specimen's thickness. Round

specimen's mesh refinement was observed in the working part of the specimen (Fig. 5b – Refined I). Handling part and transition zone of the specimen mesh was not refined (Fig. 5b – Initial).

Error distribution for refined mesh was presented in Figure 6. First refinement iterations of flat specimen decrease the error value for plane mesh elements (Fig. 6a). The error value for locked specimen's surface reach 25% of maximal error value in flat specimen (3). Highest values of the error were obtained for areas with highest plastic deformations (working part of the specimen). Considerable value of the error (25% of the maximal value) was reported near the transition zone (transition between working and handling part of the specimen). Described error distribution after first refinement was used to perform second mesh refinement iteration. Highest error values after first mesh refinement iteration was observed in working part of round specimen (Fig. 6b). Area near transition zone and area near locked surface of round specimen's mesh shows error about 25% of maximal value in the whole mesh. Maximal value of the error for round specimen's mesh after first refinement iteration is 266. For flat specimen's mesh after first refinement iteration calculated error is two times higher (514). Flat specimen's mesh after second refinement iteration was shown in Figure 7a. Areas called Initial represent mesh

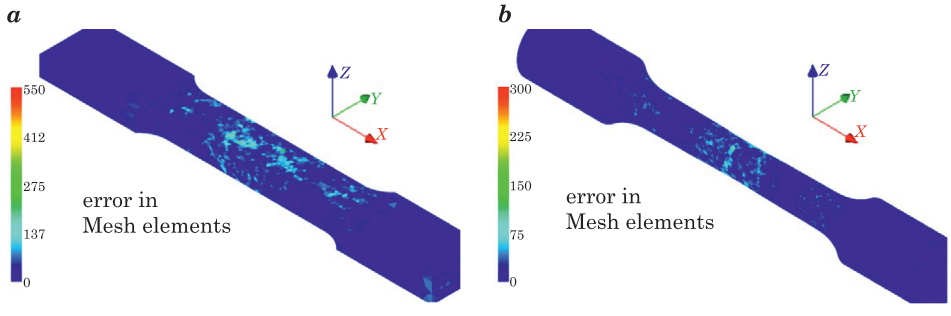

Fig. 6. Error distribution for 1 time refined mesh of *a*) flat and *b*) round specimen

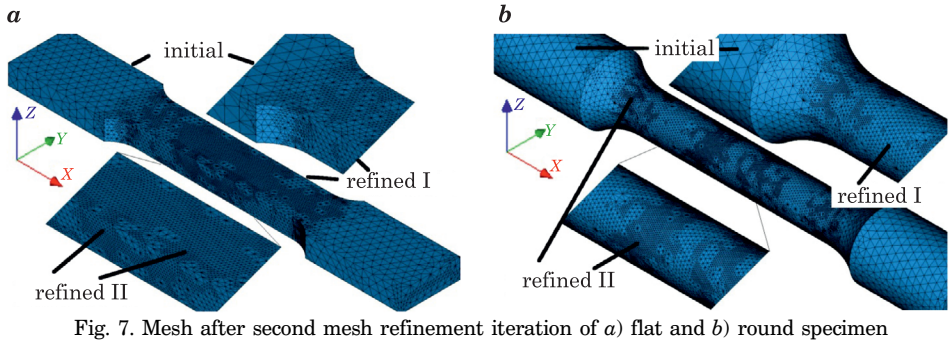

Fig. 7. Mesh after second mesh refinement iteration of *a*) flat and *b*) round specimen

before refinement. Refined I areas represent mesh not refined during second iteration. Refined II areas represent areas after both refinement iterations. Round specimen's mesh after second refinement iteration was shown in Figure 7b. Handling part of the specimen is not modified (initial mesh size).

Influence of refinement iterations on the mesh file size for flat and round tensile specimen was presented in Figure 8. First flat specimen's mesh refinement iteration has caused 8.5-fold increase of the mesh file size from 0.3 up to 2.6 MB. Second mesh refinement iteration has caused increase of the mesh file size up to 12.8 MB. This gives a 42-fold increase of the initial mesh file size. The computation time in this case was extended from 20 minutes at an initial mesh up to two hours after two flat mesh refinement iterations. The round mesh file size after first refinement iteration was increased from 0.76 up to 6.1 MB. This gives almost 8-fold increase of the file size. Second mesh refinement iteration has caused increase of the mesh file size up to 30.8 MB. This gives a 40-fold increase of the initial mesh file size. The computation time in this case was extended from 50 minutes at an initial mesh up to 32 hours after two round mesh refinement iterations. After two flat mesh refinement iterations, maximal error was 204 and 103 for round two times refined mesh. Influence of refinement iterations on the maximal error value for flat and round specimen's mesh was presented in Figure 9.

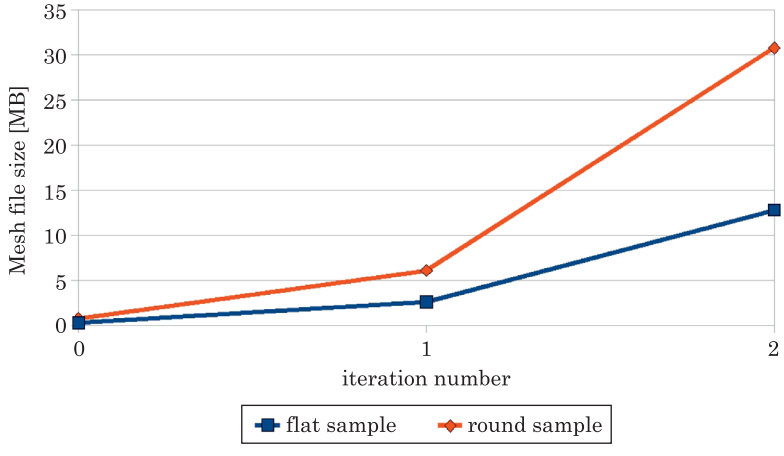

Fig. 8. Influence of mesh refinement iterations on the mesh file size

Fitting of experimental data to numerically calculate was presented as evolution of correlation coefficient value (5) for different geometries and mesh refinement iterations (Table 2). Graphical representation of fitting for initial meshes was presented in Figure 10. Double flat mesh refinement has improved fitting of numerical results to experimental data. The increase of the correlation

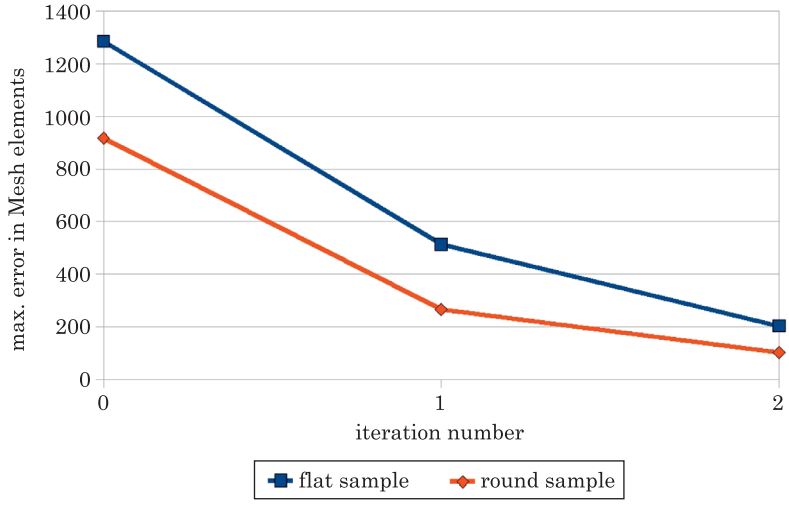

Fig. 9. Influence of mesh refinement iterations on the maximal error value in plane mesh elements

coefficient value in the analyzed range confirms this relationship. The increase of the correlation coefficient value after second flat mesh refinement iteration was 10 times lower than after first refinement. This shows smaller improvement of experimental and numerical fitting. 0.044% increase of Pearson correlation coefficient was observed after first round mesh refinement iteration. Second round mesh refinement has decreased correlation coefficient value.

Table 2

Correlation coefficient for different refinements

Iteration	Flat sample	Round sample
0	0.997654900	0.997622964
1	0.997655629	0.998062859
2	0.997655710	0.998062322

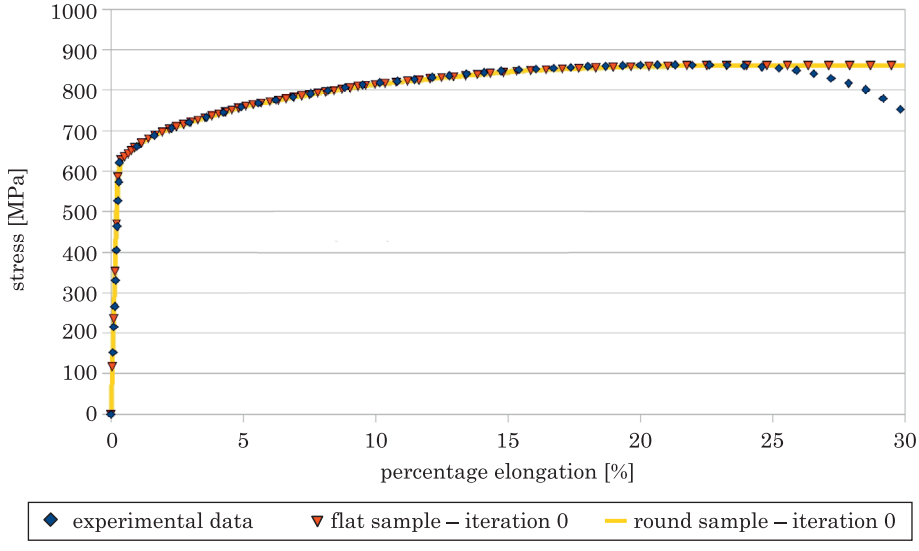

Fig. 10. Numerical and experimental tensile curve for initial meshes

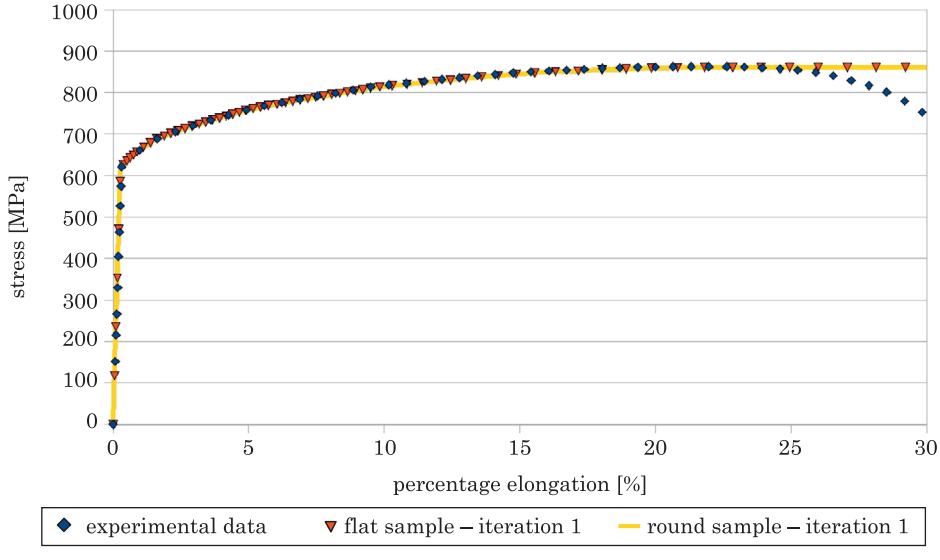

Fig. 11. Numerical and experimental tensile curve for refined mesh

For stresses 0 – UTS, results of numerical calculations coincide with experimental data. When UTS reached, numerically calculated stresses are constant and equal UTS with increasing strains. This induce difference between experimental numerically calculated stresses for percentage elongations higher

than 25%. This phenomenon was wider described in the paper (SZABRACKI et al. 2012). Small difference of correlation coefficient value between initial and refined mesh (Table 2) confirmed with negligible difference between experimental and numerically calculated results (Fig 11). Small variation of correlation coefficient value between first and second refinement iteration (Table 2) also confirmed with small differences on the tensile curve for double refined mesh (Fig. 12).

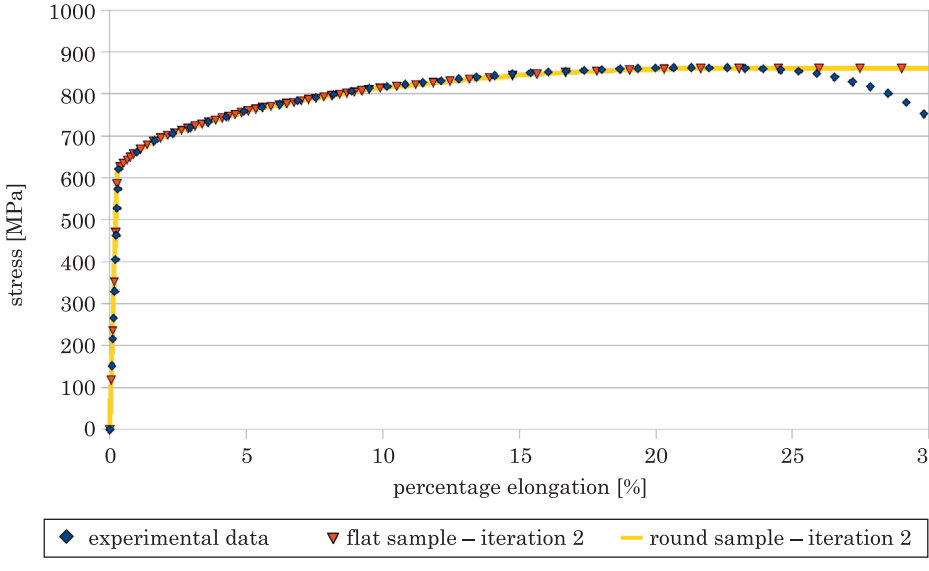

Fig. 12. Numerical and experimental tensile curve for double refined mesh

Summary

It has been shown that the local mesh refinement, performed in areas with a large error, it greatly improves the results of the fitting the experimental results with numerical results. This confirms the increase of the correlation coefficient.

Local mesh refinement allows for expansion of the mesh in areas with high error without creating unnecessary expand of the mesh in areas where error was considered to be satisfactory. This improves the matching of the results obtained at the same time and reduces the calculation time in comparison with uniform mesh refinement over the entire volume of the mesh.

Increase with ten thousandths of the correlation coefficient obtained for subsequent iterations will improve the fit too small for the analysis, and

significantly increase the computation time and computer resources needed to carry out these calculations.

First iteration of local mesh refinement performed for round and flat tensile specimens has improved fitting of numerical results to experimental data with acceptable increase of the mesh file size. Similar observations have been made for the second iteration of the flat sample local mesh refinement. Based on the analysis results have shown that second iteration of the local mesh refinement for the round specimen has increased the file size of the mesh and the computation time with slightly improved fit. There is, the limit number of iterations for which the local mesh refinement is appropriate. If the limit number of iterations was exceeded, the mesh file size and calculation time increases disproportionately to the benefits of the fitting improvement.

When error value does not exceeds about 30% of the Yield Strength no more local mesh refinement is needed. For our case, error at the level of 200–230 is acceptable for real calculations. Further refinement increase calculation costs (time and hardware) but do not improve significantly results.

Influence of local mesh refinement on the tensile test simulation results improvement was confirmed for normalized tensile specimens. This is an initial step for refinement of more complex geometries and real constructions analysis.

References

AINSWORTH M., ZHU J.Z., CRAIG A.W., ZIENKIEWICZ O.C. 1989. *Analysis of the Zienkiewicz-Zhu a-posteriori error estimator in the finite element method*. International Journal for Numerical Methods in Engineering, 28(9): 2161–2174.

ALEXA M. 2002. *Refinement operators for triangle meshes*. Computer Aided Geometric Design, 19, 169–172.

BABUSKA I., FLAHERTY J.E., HENSHAW W.D., HOPCROFT J.E., OLIGER J.E., TEZDUYAR T. 1995. *Modeling, Mesh Generation, and Adaptive Numerical Methods for Partial Differential Equations*. The IMA Volumes in Mathematics and its Applications, 75.

BABUSKA I., RHEINBOLDT W.C. 1978.*A posteriori error estimates for the finite element method.* International Journal for Numerical Methods for Engineering, 12: 1597–1615.

BÉCACHE E., JOLY P., RODRÍGUEZ J. 2005. *Space-time mesh refinement for elastodynamics. Numerical results*. Computer methods in applied mechanics and engineering, 194: 355–366.

BELL J., BERGER M., SALTZMAN J., WELCOME M. 2006. *Three-Dimensional Adaptive Mesh Refinement for Hyperbolic Conservation Laws*. SIAM Journal of Scientific Computing, 15(1): 127–138.

BERN M.W., FLAHERTY J.E., LUSKIN M. 1999. *Grid Generation and Adaptive Algorithms.* IMA Volumes in Mathematics and its Applications. Springer-Verlag New York Inc. New York.

CLARK K., FLAHERTY J.E., SHEPHARD M.S. 1994. *Applied Numerical Mathematics.* Special Issue. Adaptive Methods for Partial Differential Equations, 14.

Code–Aster. www.code-aster.org (access: 1.02.2014).

DUARTEM M., DESCOMBES S., TENAUD C., CANDEL S., MASSOT M. 2013. T*ime-space adaptive numerical methods for the simulation of combustion fronts*. Combustion and Flame, 160(6): 1083–1101.

DUMONT T., DUARTE M., DESCOMBES S., DRONNE M., MASSOT M., LOUVET V. 2013. *Simulation of human ischemic stroke in realistic 3D geometry*. Communications in Nonlinear Science and Numerical Simulation, 18(6): 1539–1557.

KŁYSZ S., SZABRACKI P., LISIECKI J. 2013. *Numeryczna symulacja testu na odporność na pękanie dla stopu aluminium stosowanego w lotnictwie*. Prace Naukowe ITWL, 32: 93–100.

KOSTOFF R.N., CUMMINGS R.M. 2013. *Highly cited literature of high-speed compressible flow research*. Aerospace Science and Technology, 26(1): 216–234.

KUHL L., BELL J.B., BECKNER V.E., BALAKRISHNAN K., ASPDEN A.J. 2013. *Spherical combustion clouds in explosions*. Shock Waves, 23(3): 233–249.

MIAZIO Ł., ZBOIŃSKI G. 2014. *hp-Adaptive finite element analysis of thin-walled structures with use of the numerical tools for detection and range assessment of boundary layers*. Recent Advances in Computational Mechanics. Taylor & Francais Group, London, pp. 57–62.

NICOLAS G., FOUQUET T. 2013. *Adaptive mesh refinement for conformal hexahedralmeshes*. Finite Elements in Analysis and Design, 67: 1–12.

PERDUTA A., PUTANOWICZ R. 2013. *Mesh Adaptation Components in FEM Framework*. 20th International Conference on Computer Methods in Mechanics, MS10, 13–14.

PN-EN ISO 6892-1. *Metallic materials – Tensile testing*. Part 1. *Method of test at room temperature*.

ROSSILLON F., MEZIERE Y. 2010. A*nalysis of fracture specimen failure of inconel 600: elastic-plastic calculations and thermo plastic energy fracture parameter*. PVP 25323.

SZABRACKI P. 2012. *Fracture behavior of nickel based alloy 600 of ductile tearing*. Tech. rep., EDF SEPTEN internal report.

SZABRACKI P., BRAMOWICZ M., LIPIŃSKI T. 2012. *Development and verication of work hardening models for X2CrNiMoN25-7-4 super duplex stainless steel after sigma phase precipitation hardening used for FEM simulations*. Journal of Power Technologies, 92(3): 166–173.

SZABRACKI P., LIPIŃSKI T. 2013. *Effect of Aging on the Microstructure and the Intergranular Corrosion Resistance of X2CrNiMoN25-7-4 Duplex Stainless Steel*. Solid State Phenomena, 203–204: 59–62.

TAYLOR J.R. 1999. *Wstęp do analizy błędu pomiarowego*. PWN, Warszawa.